Journal of Materials Science: Materials in Medicine (2018) 29:183
https://doi.org/10.1007/s10856-018-6193-7

BIOMATERIALS SYNTHESIS AND CHARACTERIZATION

Original Research

Improvement of anti-washout property of calcium phosphate cement by addition of konjac glucomannan and guar gum

Guowen Qian[1,2] · Xingmei Li[1,2] · Fupo He[3] · Jiandong Ye[1,2,4]

Received: 11 July 2018 / Accepted: 21 November 2018 / Published online: 3 December 2018

Abstracts

The inferior anti-washout property of injectable calcium phosphate cement (CPC) limits its wider application in clinic. In this study, the improvement of anti-washout performance of CPC by addition of konjac glucomannan or guar gum, which was dissolved in the CPC liquid, was first studied. The influence of KGM/GG blend with different mass ratios on the anti-washout property, compressive strength and in vitro cytocompatibility of CPC was estimated. The results revealed that small amount of KGM or GG could obviously enhance the anti-washout property of CPC. Moreover, the washout resistance efficiency of KGM/GG blend was better than KGM or GG alone. The addition of KGM/GG blend slightly shortened the final setting time of CPC. Although the introduction of KGM/GG blend reduced the compressive strength of CPC, the compressive strength still reached or surpassed that of human cancellous bone. The best KGM/GG mass ratio was 5:5, which was most efficient at not only reducing CPC disintegration, but also increasing compressive strength. The addition of KGM/GG blend obviously promoted the cells proliferation on the CPC. In short, the CPC modified by KGM/GG blend exhibited excellent anti-washout property, appropriate setting time, adequate compressive strength, and good cytocompatibility, and has the potential to be used in bone defect repair.

Graphical Abstract

The addition of KGM/GG blend significantly improved the anti-washout property of CPC. The best KGM/GG mass ratio was 5:5, which was most efficient in reducing the CPC disintegration.

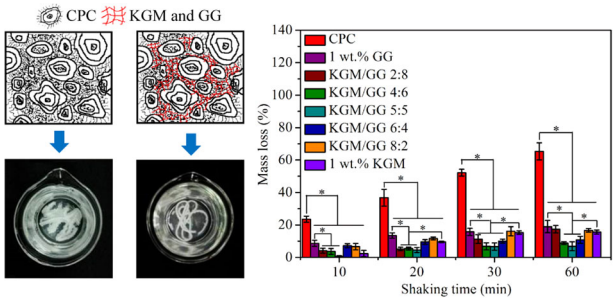

These authors contributed equally: Guowen Qian, Xingmei Li.

✉ Jiandong Ye
jdye@scut.edu.cn

[1] School of Materials Science and Engineering, South China University of Technology, 510641 Guangzhou, China

[2] National Engineering Research Center for Tissue Restoration and Reconstruction, South China University of Technology, 510006 Guangzhou, China

[3] School of Electromechanical Engineering, Guangdong University of Technology, 510006 Guangzhou, China

[4] Key Laboratory of Biomedical Materials and Engineering of the Ministry of Education, South China University of Technology, 510006 Guangzhou, China

1 Introduction

A self-setting calcium phosphate cement (CPC) was first reported by Brown and Chow [1]. CPC has been extensively studied in the last three decades and proved to be highly useful in orthopedics, maxillofacial and dentistry due to their excellent biocompatibility, good osteoconductivity, self-setting, injectability, and capacity to fill complicated-shaped defects [2–7]. However, CPC paste is prone to disintegrate by excess fluids that may be present at the surgical site [8–11]. Solid particles separated from CPC may enter into blood vessels resulting in severe inflammatory reaction, pulmonary embolism and cardiovascular diseases [12]. The poor anti-washout capacity of injectable CPC greatly limits its wider application. For this reason, a great deal of attention has been paid to improve the anti-washout property of CPC.

Enhancing cohesion and accelerating setting process of CPC paste are both direct and effective methodologies to prevent the decay of cement paste. The cohesion of CPC is commonly enhanced by the increasing viscosity of CPC liquid, which can be achieved by introducing various synthetic and natural polymers, such as modified starch [9], xanthan gum [12], cellulose derivatives [13], sodium alginate [14]. In addition, the setting time of CPC is obviously shortened by the introduction of mesoporous bioactive glass [15] and wollastonite [10]. The reduction of setting time is beneficial for the improvement of anti-washout property of CPC paste. However, many polymer-type anti-washout agents, such as modified starch, cellulose derivatives and so on, significantly prolong the setting time of CPC, which obviously limits its application in clinic [9, 13]. On the other hand, the inorganic particles used as anti-washout agents can profoundly shorten the setting time of CPC, but the improvement of anti-washout property is not obvious enough and large amount of inorganic particles should be added in most cases [10, 15].

Konjac glucomannan (KGM) is a water-soluble and non-ionic neutral natural polysaccharide derived from the tuber of Amorphophallus konjac C. Koch [16, 17]. KGM consists of β-1, 4 linked glucose and mannose units [18]. In general, KGM loses acetyl groups in alkaline environment, then its molecules aggregate in part with one another by the role of hydrogen bonds leading to the formation of the gel network structure [19]. KGM is a nontoxic, biocompatible and common dietary ingredient [16]. KGM also has high molecular weight, strong hydration capacity and good thickening performance. Therefore, KGM has been used widely in drug delivery, medical dressing and bone repair materials.

Guar gum (GG) is also a natural plant polysaccharide consisted of D-mannose residues connected by glycosidic bonds, and it can be obtained from the seeds of the legume cyamopsis tetragonalobus [20]. β-D-mannopyranose units with α-D-glactopyranose units are connected with the mannose backbone by glycosidic bonds [21]. GG is water-soluble, nontoxicity, and able to control the release of drugs, hence GG has been broadly used in the pharmaceutical field [20]. GG also has excellent thickening effect, which is 5-8 times higher than that of starch.

KGM and GG both have excellent thickening performance, which make them promising anti-washout agents for CPC. It is speculated that the hybrid system will form much stronger composite gel than KGM or GG used alone. To the best of our knowledge, there is no published work regarding improvement of the anti-washout property of CPC with KGM/GG blend.

In this study, we have first studied the effects of addition amount of KGM or GG alone and then the KGM/GG blend with different mass ratios on the washout performance of CPC. The physiochemical and cellular behaviors of the CPC with these viscous additives were also systemically investigated.

2 Materials and methods

2.1 Materials

$Ca(NO_3)_2{\cdot}4H_2O$, $Na_2HPO_4{\cdot}12H_2O$, $CaHPO_4{\cdot}2H_2O$, anhydrous ethanol, and guar gum were commercially obtained from Aladdin's Reagent (Shanghai) Co., Ltd. Konjac glucomannan (KGM) was bought from Beijing Bioco Laibo Technology Co. Ltd. All the commercial chemicals were analytically pure. Cell-culture related reagents were purchased from Gibco (Invitrogen, USA) except specialized.

2.2 Material preparations

The CPC powder used in this study was a mixture of partially crystallized calcium phosphate (PCCP) and dicalcium phosphate anhydrous ($CaHPO_4$, DCPA) as introduced in the previous work of our research group [22]. In brief, PCCP was synthesized from an aqueous solution of $Ca(NO_3)_2{\cdot}4H_2O$ and $Na_2HPO_4{\cdot}12H_2O$ by chemical precipitation method. Then the precipitate was centrifugally separated, freeze-dried, and heat treatment at 460 °C for 2 h in a furnace. DCPA powder was obtained by milling $CaHPO_4{\cdot}2H_2O$ in ethanol for 2 h and then dried at 120 °C for 12 h.

Certain amounts of KGM and/or GG were added to deionized water, then a series of homogeneous solutions at the concentrations of 0.5, 1.0 and 2.0 wt.% were obtained

after stirring at 50 °C for 20 min. The cement pastes were obtained by homogeneously mixing CPC powder with KGM solutions (0, 0.5, 1.0, 2.0 wt.%) or GG solutions (0, 0.5, 1.0, 2.0 wt.%) at a liquid to powder ratio of 0.4 mL/g.

In order to study the combinatory effect of KGM and GG on the overall performance of CPC. Various KGM/GG blend solutions (1 wt.%) were prepared to be used as setting liquid of CPC. The KGM/GG mass ratio of blend solution was set at 2:8, 4:6, 5:5, 6:4, 8:2, respectively. The cement pastes were prepared by mixing CPC powder with KGM/GG blend solutions at a liquid to powder ratio of 0.4 mL/g.

2.3 Anti-washout property evaluation

The weight (M_0) of CPC powders was weighed. After mixing with CPC liquid, the as-prepared consistency cement pastes were poured into a disposable syringe without nozzle. Then, the pastes were immediately injected into simulated body fluid (SBF, 30 mL) solution and shaken at 60 rpm for 0, 15, and 30 min. The SBF was prepared according to the method described by Kokubo [23]. The anti-washout property of the cement pastes was visually evaluated via the extent of decay of the pastes [8]. For quantitative measurement, the CPC pastes were poured into stainless steel molds. Subsequently, the cylindrical cement specimens (6 mm in diameter and 12 mm in height) were immediately demoulded and soaked in SBF solution (30 mL for each) and shaken at 60 rpm for 0, 10, 20, 30, and 60 min. Then the samples were taken out at designed points and dried at 37 °C. After that, the weight (M_1) of samples was measured. The decay amounts of the cements were evaluated according to (1).

$$\text{Mass loss}\,(\%) = (M_0 - M_1)/M_0 \quad (1)$$

2.4 Viscosity test

Viscosity of the CPC paste was tested by a rheometer (ARG2, TA Instrument, USA). The liquid to powder ratio of CPC was adjusted to 1 mL/g due to the limitation of the rheometer. The viscosity curves were obtained by measuring the variation of viscosity with shear rate (0.01-100 s^{-1}).

2.5 Setting time measurement

The setting time of each sample was measured by Gilmore needle method according to ISO standard (9917–1:2007 (E)). The CPC paste was filled into a mold (12 mm in diameter and 2 mm in height). To measure the initial setting time, a 'lighter' Gilmore needle (2.12 mm in diameter and 113.4 g of weight) was dropped onto the surface of the sample and stayed for 5 s in every 1 minute, and the setting time was recorded until the needle tip no longer made an obvious indentation on the surface of CPC. To measure the final setting time, a 'heavier' Gilmore needle (1.06 mm in diameter and 453.6 g of weight) was dropped onto the surface of the sample and stayed for 5 s in every 2 minutes, the setting time was recorded until the needle tip did not make an obvious indentation on the surface of CPC.

2.6 Compressive strength test

The CPC pastes were filled into molds (6 mm in inner diameter, 12 mm in height) and pressed by using a press machine (HLD, HANDPI, China) under a 10 kg force for 15 s to remove the bubbles in paste. After demoulded, the samples were incubated at 37 °C and 98% humidified atmosphere for 3 days, and then dried at 80 °C. The obtained CPC samples were tested on compressive strength by using a universal material testing machine (Instron 5567, Instron, USA) at the crosshead speed of 1 mm min^{-1}.

2.7 Porosity measurement

The preparation of the samples for porosity measurement is the same as that for compressive strength test. Porosity of CPC samples was measured using a density balance (FA1104J, China) according to Archimedes principle. First, the dry weight (W_0) of samples was weighed, then the samples were soaked in anhydrous ethyl alcohol under vacuum (< 0.08 MPa) for 2 h to ensure the infiltration of ethanol into the pores of CPC. Second, the weight (W_1) of wet samples was measured after wiping alcohol on their surface with a gauze saturated by alcohol. Finally, the weight (W_2) of samples in the alcohol was weighed. The porosity of samples was calculated according to the equation (2).

$$\text{Porosity} = (W_1 - W_0)/(W_1 - W_2) \times 100\% \quad (2)$$

2.8 Phase and microstructure characterization

The hydrated samples were grinded into powders, and then the phase of powdered samples was determined employing an X-ray diffractometer (XRD, X'Pert PRO, PANalytical, Netherlands) with Cu-K_α radiation. The XRD patterns were collected in the 2θ range of 10° to 70° with a step size of 0.013°. Prior to SEM observation, the samples were sputter-coated with gold. Microstructure of the fractured surface of samples were observed by using a scanning electron microscope (SEM, Nova NanoSEM 430, FEI, Netherlands) with an accelerating voltage of 15 kV.

2.9 Cytocompatibility assessment

2.9.1 Cell culture

Mouse bone marrow mesenchymal stem cells (mBMSCs, ATCC, USA) were cultured in cell culture flasks with complete culture medium in an incubator (37 °C, 5% CO_2). The complete culture medium was consisted of 90 vol.% high-glucose Dulbecco's modified eagle's medium (H-DMEM) and 10 vol.% fetal bovine serum (FBS). The medium were refreshed every 2 days.

2.9.2 Cell attachment and morphology

The cement disks (6 mm in diameter and 1.5 mm in height) were sterilized by γ irradiation at 15 kGy. The disks were placed in a 48-well plate. Subsequently, 2×10^4 cells/mL cell suspension (0.5 mL/well) was seeded on the disks. After 1 day of incubation, the specimens were washed 3 times with phosphate buffer solution (PBS), fixed with 2.5% glutaraldehyde solution for 24 h, dehydrated with gradient ethanol (30 vol.%, 50 vol.%, 70 vol.%, 80 vol.%, 90 vol.%, 95 vol.%, and 100 vol.%) and air-dried. Finally, the morphology of cells attached on the cement disks were observed by using a scanning electron microscope (SEM, Nova NanoSEM 430, FEI, Netherlands) with an accelerating voltage of 15 kV.

2.9.3 Fluorescent labeling of live/dead assay

The viability and cytotoxicity of mBMSCs cultured on the cement disks were characterized by using Live-Dead Cell Staining Kits (Biotium, No. 30002, USA) following manufacturer's instructions. Briefly, the disks were transferred into a new 48-well plate and washed twice with PBS gently after being cultured for 24 h. Then, 250 μL PBS working solution containing 2 mM calcein AM (labeling live cells) and 4 mM EthD-III (labeling dead cells) was added, then incubated at 37 °C for 45 min under the dark condition. Finally, the working solution was sucked out, and the disks were washed twice with PBS gently and observed under a fluorescence inverted microscope (Nikon, Eclipse Ti-U, Japan).

2.9.4 Cell proliferation

The CPC disks were placed into 48-well plates and cell suspensions (500 μL, 2×10^4 cells/mL) was added to each well. After cell culture for 1, 3, and 7 days, Cell Counting Kit-8 (CCK-8, Dojindo Laboratories, Japan) was used to

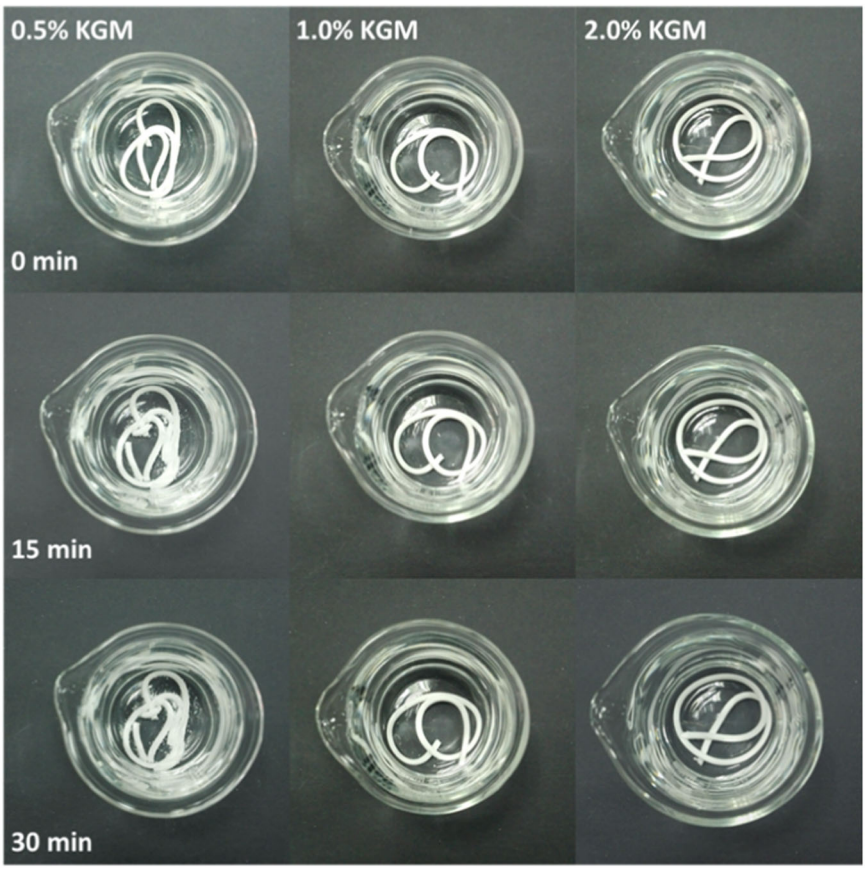

Fig. 1 Anti-washout observation of the cement pastes with different KGM contents in SBF after being shaken for 0, 15, and 30 min

evaluate the proliferation of mBMSCs on the disks according to manufacturer's instructions. In brief, the disks were transferred to a new 48-well plate. Then, the complete culture medium (250 μL) containing 10 vol% CCK-8 work solution was added to each well and the cell-sample constructs were incubated at 37 °C for 1 h. The absorbance of supernatant was read at 450 nm by using a microplate reader (Thermo 3001, USA).

2.10 Statistical analysis

All data in this study were repeated at least three times and presented as mean value ± standard deviation (SD). Student's *t*-test was performed to analyze differences between experimental groups. A value of $p < 0.05$ was regarded as statistical significance ($^{*}p < 0.05$, $^{**}p < 0.01$, $^{***}p < 0.001$).

3 Results

3.1 Optimization of KGM and GG concentration

Figure 1 exhibits the visual anti-washout inspection of the cement pastes with different KGM contents in SBF after being shaken for 0, 15, and 30 min. When the content of KGM was 0.5 wt.%, a small amount of the cement pastes was disintegrated after being shaken for 30 min. For the groups with 1.0 and 2.0 wt.% KGM, the cylindrical pastes kept well-defined shape, and there was no obvious disintegrated cement powders in SBF solution. Figure 2 shows the visual anti-washout inspection of the cement pastes with different GG contents. It is evident that the decay amount of the cement pastes decreased obviously with the increase of GG content. Like KGM groups, a lot of cement pastes with 0.5 wt.% GG were disintegrated after being shaken for 30 min; On the contrary, just a few particles were separated from the cement pastes containing 1.0 and 2.0 wt.% GG. The washout resistance efficacy of KGM is superior to that of GG at the same concentration.

From the above anti-washout results of the cement pastes, it is inferred that the anti-washout property of the cement paste increased with the increase of KGM or GG contents. To avoid affecting other properties of CPC after the addition of excessive polysaccharides, 1.0 wt.% was selected as the appropriate addition content of KGM or GG for follow-up study.

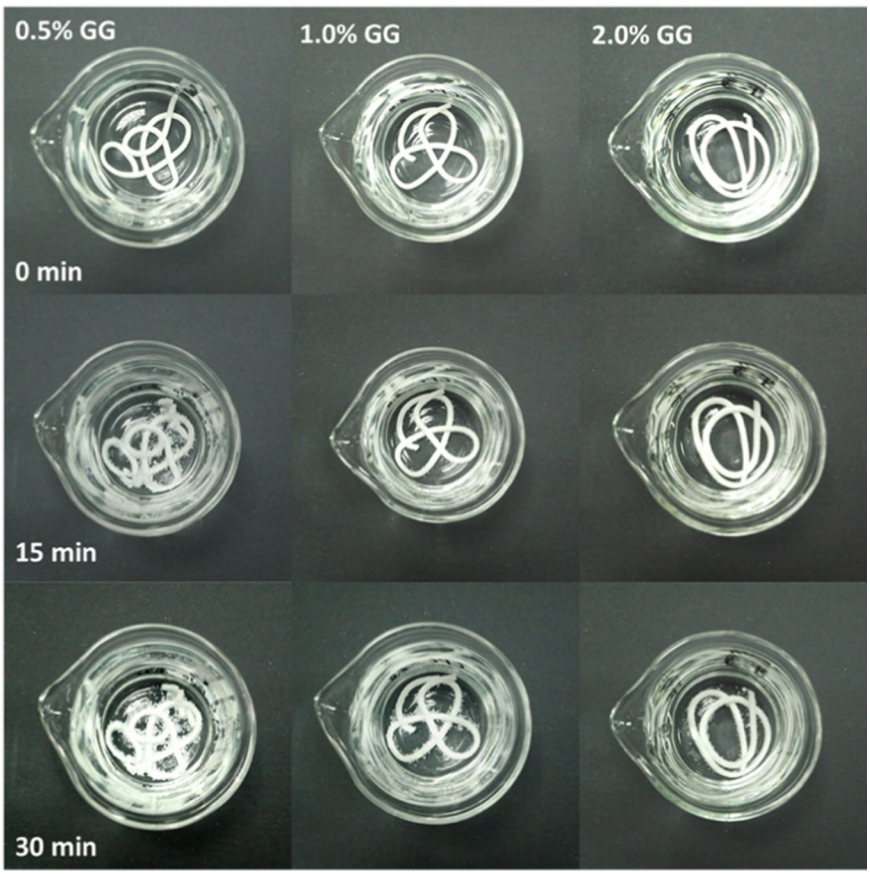

Fig. 2 Anti-washout observation of the cement pastes with different GG contents in SBF after being shaken for 0, 15, and 30 min

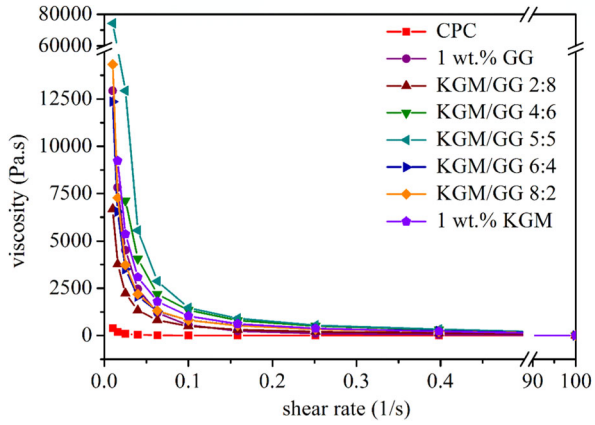

Fig. 3 Influence of KGM/GG mass ratios on the viscosity of the cement pastes

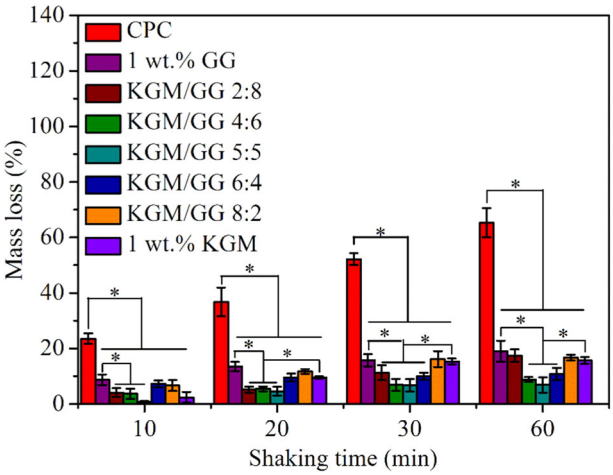

Fig. 5 Mass loss of the cement pastes containing KGM/GG blend with different mass ratios after immersion in SBF for 10, 20, 30, 60 min

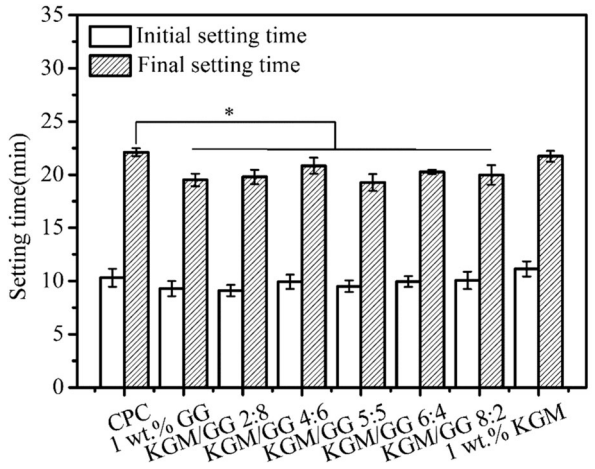

Fig. 4 The setting time of the CPC containing KGM/GG blend with different mass ratios

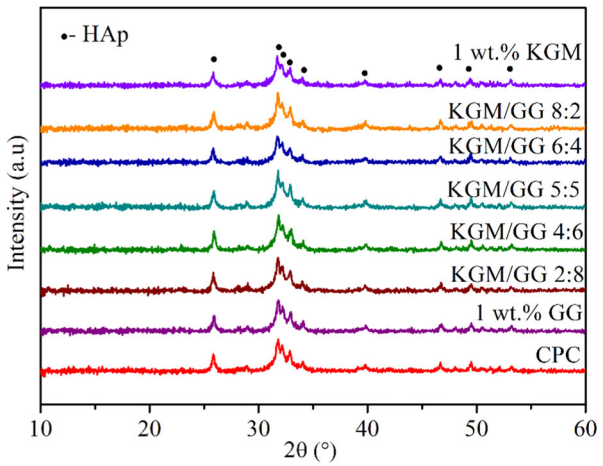

Fig. 6 XRD patterns of the CPC containing KGM/GG blend with different mass ratios

3.2 Viscosity of the CPC modified with KGM/GG blend

The viscosity of the cement pastes at different KGM/GG mass ratios is plotted in Fig. 3. The viscosity of all cement pastes decreased with the increase of shear rate, demonstrating that the CPC slurry is a non-Newtonian fluid featured with the phenomena of shear thinning. The addition of 1 wt.% GG or KGM alone significantly enhanced the viscosity of the cement pastes in comparison to the CPC without additive. Moreover, the viscosity of the cement pastes with 1 wt.% KGM was higher than that with 1 wt.% GG at the same shear rate. The viscosity of the pastes increased first and then decreased with increasing mass ratio of KGM to GG. It should be noted that the highest viscosity was shown in the cement pastes as introducing KGM/GG blend at KGM to GG ratio of 5:5.

3.3 Setting time of the CPC modified with KGM/GG blend

Figure 4 shows the influence of different KGM/GG mass ratios on the setting time of the CPC. The initial setting time of all samples was about 10 min, which was no distinct difference between each other. However, the addition of KGM/GG blend whatever the mass ratios shortened the final setting time of CPC.

3.4 Anti-washout property of the CPC modified with KGM/GG blend

Figure 5 displays the quantitative results of the anti-washout property of the cement pastes containing KGM/GG blend with different mass ratios. It can be seen that the cement pastes decayed gradually with the prolongation of shaking time. The sample without anti-washout additive decayed

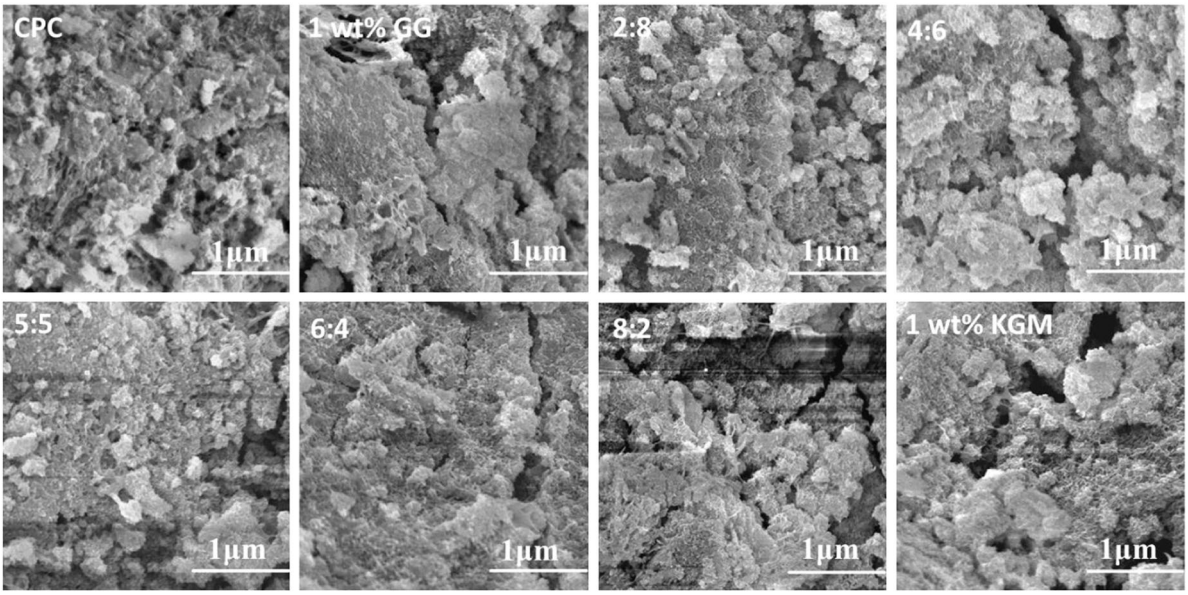

Fig. 7 SEM micrographs of fracture surface of the CPC containing KGM/GG blend with different mass ratios

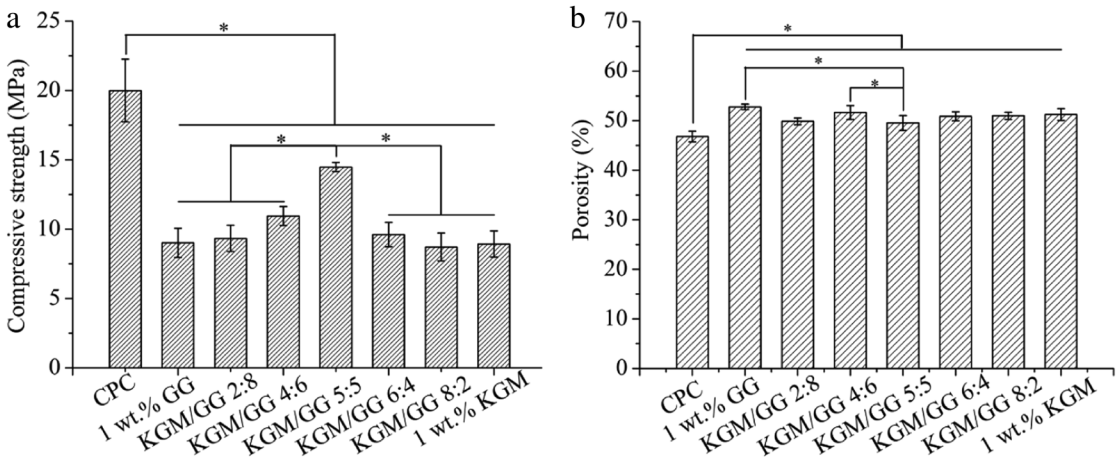

Fig. 8 Compressive strength **a** and porosity **b** of the CPC containing KGM/GG blend with different mass ratios

fast and its mass loss reached 63.26% ± 2.95% after being shaken in SBF for 60 min. By contrast, CPC with 1 wt.% KGM or 1 wt.% GG did not decay obviously during shaking. Furthermore, CPC modified by KGM/GG blend showed better anti-washout effect than that with KGM or GG alone. When the KGM/GG mass ratio was 5:5, the obtained cement paste showed the lowest mass loss, whereas further increase of the KGM/GG mass ratio led to the increased mass loss of the cement pastes slightly. Within 60 min, the CPC modified with 1 wt.% GG and 1 wt.% KGM had mass loss of 19.00% and 15.60%, respectively, while CPC containing KGM/GG blend (KGM/GG mass ratio of 5:5) decayed only 6.88%.

3.5 Phase and microstructure

Figure 6 shows XRD patterns of the cements containing KGM/GG blend with different mass ratios after hydration for 3 days. The characteristic peaks of hydroxyapatite (HA, JCPDS 00-009-0432) can be seen from the XRD patterns of all samples. There was no obvious difference among the XRD patterns of the different groups. Figure 7 presents SEM photographs of fractured surface of the CPC containing KGM/GG blend with different mass ratios. A lot of tiny needle-like and plate-like apatite grains interlocked with each other and plentiful nano and submicron pores with irregular shapes were observed in the CPC.

3.6 Compressive strength and porosity

Figure 8a exhibits the effect of different KGM/GG mass ratios on the compressive strength of CPC. The addition of polysaccharides decreased the compressive strength of the cement. The compressive strength of CPC without anti-washout additive was about 19.99 MPa, while the compressive strength of CPC with 1 wt.% GG and 1 wt.% KGM was about 9.01 MPa and 8.93 MPa, respectively. The compressive strength of CPC was also affected by the KGM/GG mass ratio. When the KGM/GG mass ratio was lower than 5:5, the compressive strength was improved with increasing mass ratio of KGM/GG. The cement with the KGM/GG mass ratio of 5:5 had the highest compressive strength (14.48 ± 0.33 MPa). The compressive strength of the CPC correspondingly reduced when the KGM/GG mass ratio was above 5:5. As shown in Fig. 8b, the addition of KGM/GG blend obviously increased the porosity of CPC.

3.7 In vitro cytocompatibility

Figure 9 presents the morphology of mBMSCs attached on the surface of the CPC disks containing KGM/GG blend with different mass ratios after culture for 1 day. The cells completely spread on all the samples with obvious pseudopodium. Figure 10 displays the viability of mBMSCs on the CPC disks containing KGM/GG blend with different mass ratios. After 3 days of cell culture, a plenty of green-fluorescent viable cells attached on the surface of all samples, only a few red-fluorescent necrotic or apoptotic cells were observed. The cell proliferation on the CPC samples with KGM/GG blend is showed in Fig. 11. The cells

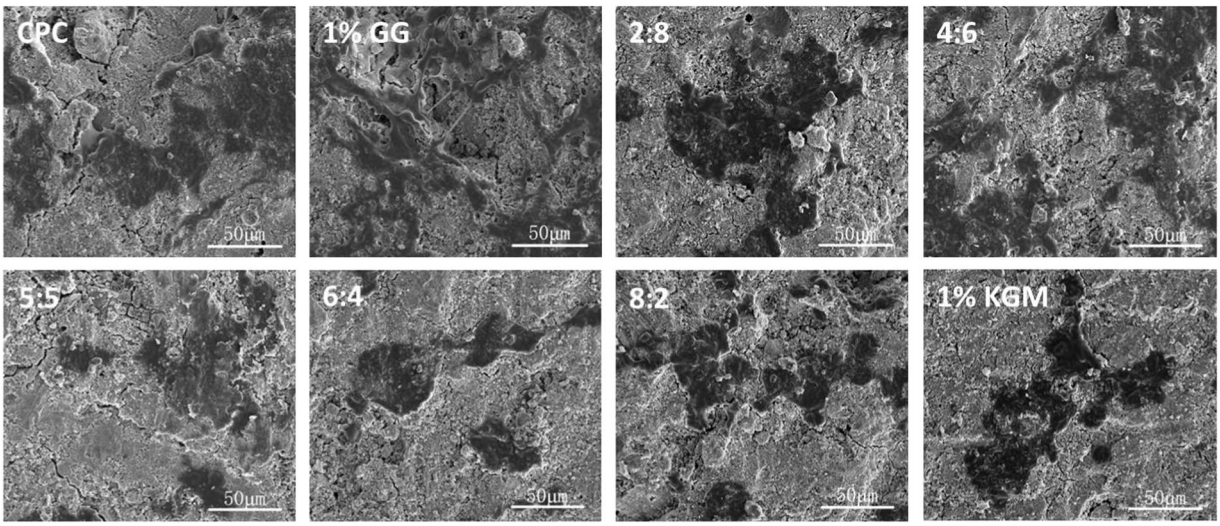

Fig. 9 SEM images of the attachment morphology of mBMSCs cultured on the surfaces of CPC disks containing KGM/GG blend with different mass ratios

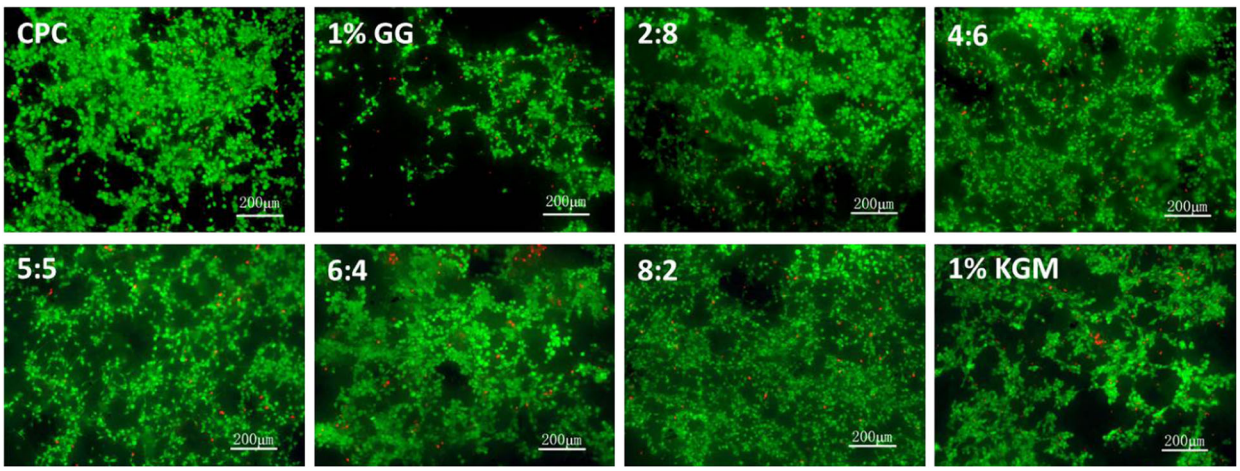

Fig. 10 Fluorescence photos of Live/Dead mBMSCs cultured on CPC disks containing KGM/GG blend with different mass ratios

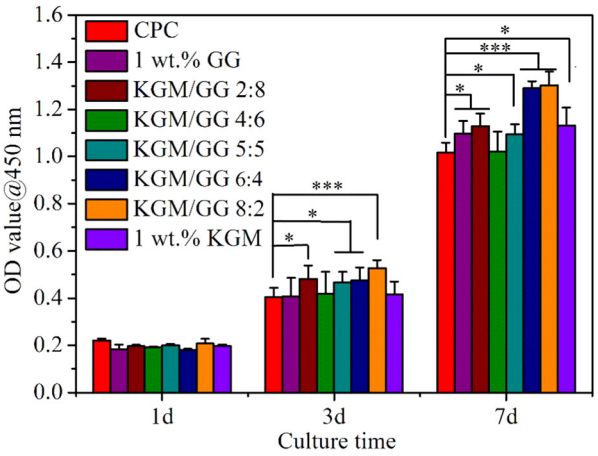

Fig. 11 Proliferation of mBMSCs cultured on the CPC disks containing KGM/GG blend with different mass ratios

gradually proliferated throughout the whole cell culture period. The addition of anti-washout additives promoted mBMSCs proliferation obviously compared to the CPC without additives.

4 Discussion

Although CPC has excellent biocompatibility and good osteoconductivity, the inferior anti-washout property of CPC limits its wider application in clinic. Our results indicated the addition of KGM and/or GG could obviously improve the anti-washout property. Moreover, the washout resistance efficiency of KGM/GG blend was better than KGM or GG alone. The best KGM/GG mass ratio was 5:5, which was most efficient at reducing CPC disintegration. The possible anti-washout mechanisms of KGM and GG could be mainly summarized on two aspects. On the one hand, the formation of strong intermolecular hydrogen bonds between two polysaccharides leads to produce three dimensional gel network structure in the cement liquid, which plays the roles of restricting and covering the CPC particles. On the other hand, KGM and GG can synergistically enhance viscosity of the cement liquid phase (Fig. 3), the improved viscosity of the cement pastes was beneficial to the increase of cohesion of CPC particles, which can protect the cement pastes from eroding and decay of surrounding liquid, thus improving the anti-washout property of CPC.

The addition of KGM/GG blend shortened the final setting time of CPC. The probable reason was the high water retention of KGM and/or GG polysaccharide molecules; these polysaccharide molecules adsorbed part of water, thus reducing water participating in dissolution-precipitation reaction, increasing of oversaturation of ions and accelerating hydration reaction process. On the other hand, KGM and GG are all macromolecules, which can enhance the viscosity of liquid phase after being dissolved (Fig. 3), leading to the increase of cohesion and close contact of the cement particles.

Hydroxyapatite (HA) crystals in CPC gradually grow and form interlocked network during the process of hydration reaction to ensure the mechanical strength of hardened CPC [6]. The addition of polysaccharides decreased the compressive strength of the cement. Moreover, the compressive strength of CPC was also affected by the KGM/GG mass ratio. When the KGM/GG mass ratio was lower than 5:5, the compressive strength was improved with increasing mass ratio of KGM/GG. The cement with the KGM/GG mass ratio of 5:5 had the highest compressive strength. The strength of the CPC correspondingly reduced when the KGM/GG mass ratio was above 5:5. The mechanical strength of CPC is tightly associated with the microstructure of CPC, such as porosity [24], pore size [25], and so on. A lot of small pores form during the hydration process of CPC [22], and the porosity is one of the important factors which influences the mechanical strength and biological performance of CPC [24, 26]. Figure 8b illustrates the porosity of CPC containing KGM/GG blend with different mass ratios. It can be seen that the porosity of CPC without additive was a little lower than that of the samples with anti-washout additives, which was probable one of factors resulting in the relative low compressive strength after the addition of polysaccharides. On the other hand, the dimensional gel networks formed by the polysaccharide molecules may impair the bonding strength among the inorganic crystals and reduce the mechanical strength of the hydrated CPC. The variation of compressive strength of the CPC containing KGM/GG blend with different mass ratios probably was due to the variation of the polysaccharide gel strength with different KGM/GG ratios. It was reported that the compressive strength values of human trabecular bone range from 0.10 to 27.3 MPa [27, 28]. Although the addition of KGM/GG blend reduced the strength of CPC, the compressive strength of CPC with KGM/GG blend still reached or surpassed the compressive strength range of human cancellous bone.

KGM and GG are nontoxic as natural polysaccharide, which were widely applied in food additives, supplementary materials and drug delivery. The addition of KGM/GG blend obviously promoted mBMSCs proliferation compared to the CPC without additives. It was reported that bone mesenchymal stem cells adhered preferentially to the KGM and KGM/chitosan scaffolds than the bulk films, KGM contributed to improve the biocompatibility of chitosan material [29]. Due to its good ability of supporting cells adhesion and proliferation, GG was used to prepare scaffold for tissue engineering application [30, 31]. The

KGM and/or GG at a small amount could dramatically enhance the anti-washout property of CPC. Moreover, the addition of KGM/GG blend slightly shortened the final setting time of CPC. In spite of this, the final setting time of CPC modified by KGM/GG still reached about 20 min, which is suitable to the application in clinic. Therefore, CPC modified by KGM/GG blend exhibits many advantages for bone defect repair in clinic.

5 Conclusions

In this study, the KGM/GG blend with various mass ratios was used to improve the anti-washout property of the CPC pastes. The results revealed that KGM or GG alone greatly enhanced the anti-washout property of CPC, and the washout resistance of the CPC pastes increased with increasing content of KGM or GG. The washout resistance effect of KGM/GG blend for CPC was better than that of KGM or GG alone. Moreover, efficiency of KGM/GG blend in improving bone cement cohesion is dependent on their mass ratio. The KGM/GG mass ratio of 5:5 is most efficient in reducing CPC disintegration. The addition of KGM/GG blend shortened the final setting time of CPC. The introduction of KGM/GG blend reduced the compressive strength of CPC, but it is still higher than that of cancellous bone. The modified CPC with KGM and GG showed good cytocompatibility. The addition of KGM/GG blend obviously promoted mBMSCs proliferation on the CPC. We concluded that KGM/GG blend is very effective additive for improving the anti-washout property of CPC, and the CPC modified by KGM/GG blend has the potential to be used in bone defect repair.

Acknowledgements This research was supported by the National Natural Science Foundation of China under Grant No. 51672087, the Science and Technology Program of Guangzhou City of China under Grant No. 201508020017, and the Fundamental Research Funds for the Central Universities. The authors declare that they have no conflict of interest.

Compliance with ethical standards

Conflict of interest The authors declare that they have no conflict of interest.

References

1. Brown WE, Chow LC. A new calcium phosphate, water-setting cement. Cements research progress. Wester Westerville, OH: American Ceramic Society; 1986. pp. 352–79.
2. Fernández E, Gil FJ, Ginebra MP, Driessens FCM, Planell JA, Best SM. Calcium phosphate bone cements for clinical applications, Part I. Solution chemistry. J Mater Sci Mater Med. 1999;10:169–76.
3. Fernández E, Gil FJ, Ginebra MP, Driessens FCM, Planell JA, Best SM. Calcium phosphate bone cements for clinical applications. Part II: Precipitate formation during setting reactions. J Mater Sci Mater Med. 1999;10:177–83.
4. Wang XH, Ma JB, Wang YN, He BL. Bone repair in radii and tibias of rabbits with phosphorylated chitosan reinforced calcium phosphate cements. Biomaterials. 2002;23:4167–76.
5. Guo DG, Xu KW, Zhao XY, Han Y. Development of a strontium-containing hydroxyapatite bone cement. Biomaterials. 2005;26:4073–83.
6. Wang XP, Ye JD, Wang YJ, Wu XP, Bai B. Control of crystallinity of hydrated products in a calcium phosphate bone cement. J Biomed Mater Res Part A. 2007;81A:781–90.
7. Qi XP, Ye JD, Wang YJ. Improved injectability and *in vitro* degradation of a calcium phosphate cement containing poly(lactide-co-glycolide) microspheres. Acta Biomater. 2008;4:1837–45.
8. Li XM, He FP, Ye JD. Preparation, characterization and *in vitro* cell performance of anti-washout calcium phosphate cement modified by sodium polyacrylate. RSC Adv. 2017;7:32842–49.
9. Wang XP, Chen L, Xiang H, Ye JD. Influence of anti-washout agents on the rheological properties and injectability of a calcium phosphate cement. J Biomed Mater Res Part B Appl Biomater. 2007;81B:410–8.
10. Liu JQ, Li JY, Ye JD, He FP. Setting behavior, mechanical property and biocompatibility of anti-washout wollastonite/calcium phosphate composite cement. Ceram Int. 2016;42:13670–81.
11. Liu JQ, Li JY, Ye JD. Properties and cytocompatibility of anti-washout calcium phosphate cement by introducing locust bean gum. J Mater Sci Technol. 2016;32:1021–6.
12. Chen FP, Song ZY, Liu CS. Fast setting and anti-washout injectable calcium–magnesium phosphate cement for minimally invasive treatment of bone defects. J Mater Chem B. 2015;3:9173–81.
13. Cherng A, Takagi S, Chow LC. Effects of hydroxypropyl methylcellulose and other gelling agents on the handling properties of calcium phosphate cement. J Biomed Mater Res. 1995;35:273–7.
14. Ishikawa K, Miyamoto Y, Kon M, Nagayama M, Asaoka K. Non-decay type fast-setting calcium phosphate cement: composite with sodium alginate. Biomaterials. 1995;16:527–32.
15. El-Fiqi A, Kim JH, Perez RA, Kim HW. Novel bioactive nanocomposite cement formulations with potential properties: incorporation of the nanoparticle form of mesoporous bioactive glass into calcium phosphate cements. J Mater Chem B. 2015;7:1321–34.
16. Huang L, Takahashi R, Kobayashi S, Kawase T, Nishinari K. Gelation behavior of native and acetylated konjac glucomannan. Biomacromolecules. 2002;3:1296–303.
17. Yoshimura M, Takaya T, Nishinari K. Rheological studies on mixtures of corn starch and konjac-glucomannan. Carbohyd Polym. 1997;35:71–9.
18. Nishinari K, Williams PA, Phillips GO. Review of the physico-chemical characteristics and properties of konjac mannan. Food Hydrocoll. 1992;6:199–222.
19. Maekaji K. Determination of acidic component of konjac mannan. Agric Biol Chem. 1978;42:177–8.
20. Zhang FS, Shen YD, Ren T, Wang L, Su Y. Synthesis of 2-alkenyl-3-butoxypropyl guar gum with enhanced rheological properties. Int J Biol Macromol. 2017;97:317–22.
21. Vijayendran BR, Bone T. Absolute molecular weight and molecular weight distribution of guar by size exclusion chromatography and low-angle laser light scattering. Carbohyd Polym. 1984;4:299–313.
22. Wang XP, Ye JD, Wang YJ. Hydration mechanism of a novel PCCP + DCPA cement system. J Mater Sci Mater Med. 2008;19:813–16.

23. Kokubo T, Takadama H. How useful is SBF in predicting *in vivo* bone bioactivity. Biomaterials. 2006;27:2907–15.
24. Barralet JE, Gaunt T, Wright AJ, Gibson IR, Knowles JC. Effect of porosity reduction by compaction on compressive strength and microstructure of calcium phosphate cement. J Biomed Mater Res. 2001;63:1–9.
25. Bose S, Darsell J, Kintner M, Hosick H, Bandyopadhyay A. Pore size and pore volume effects on alumina and TCP ceramic scaffolds. Mat Sci Eng C-Mater. 2003;23:479–86.
26. Chen ZT, Ni SY, Han SG, Crawford R, Lu S, Wei F, Chang J, Wu CT, Xiao Y. Nanoporous microstructures mediate osteogenesis by modulating the osteo-immune response of macrophages. Nanoscale. 2017;9:706–18.
27. Langer R, Tirrell DA. Designing materials for biology and medicine. Nature. 2004;428:487–92.
28. Lotz JC, Gehart TN, Hayes WC. Mechanical properties of trabecular bone from the proximal femur: a quantitative CT study. J Comput Assist Tomogr. 1990;14:107–14.
29. Nie HR, Shen XX, Zhou ZH, Jiang QS, Chen YW, Xie A, Wang Y, Han CC. Electrospinning and characterization of konjac glucomannan/chitosan nanofibrous scaffolds favoring the growth of bone mesenchymal stem cells. Carbohyd Polym. 2011;85:681–6.
30. Kundu S, Das A, Basu A, Ghosh D, Datta P, Mukherjee A. Carboxymethyl guar gum synthesis in homogeneous phase and macroporous 3D scaffolds design for tissue engineering. Carbohyd Polym. 2018;191:71–8.
31. Tiwari A, Grailer JJ, Pilla S, Steeber DA, Gong SQ. Biodegradable hydrogels based on novel photopolymerizable guar gum–methacrylate macromonomers for in situ fabrication of tissue engineering scaffolds. Acta Biomater. 2009;5:441–3452.